Proceedings of IPACK03
International Electronic Packaging Technical Conference and Exhibition
July 6-11, 2003, Maui, Hawaii, USA

IPACK2003-35136

WIRE FLEXURE FATIGUE MODEL FOR ASYMMETRIC BOND HEIGHT

Karumbu Nathan Meyyappan
CALCE Electronic Products and Systems Center
University of Maryland
College Park, MD 20742

Peter Hansen
Grundfos Management A/S
Poul Due Jensens Vej 7
8850 Bjerringbro, Denmark

Patrick McCluskey
CALCE Electronic Products and Systems Center
University of Maryland
College Park, MD 20742

ABSTRACT

This paper presents the first physics-of-failure based life prediction model for flexural failure of wires ultrasonically wedge bonded to pads at different heights. The life prediction model consists of a load transformation model and a damage model. The load transformation model determines the cyclic strain at the heel of the wire during temperature cycling. This cyclic strain is created by a change in wire curvature at the heel of the wire resulting from expansion of the wire and displacement of the frame. The damage model calculates the life based on the strain cycle magnitude and the elastic-plastic fatigue response of the wire. The model supports virtual qualification of power modules where wire flexural fatigue is a dominant failure mechanism. The model has been validated using temperature cycling test results, and can be used to derive design guidelines and establish a relation between accelerated test results and field life.

INTRODUCTION

Solid-state power modules, such as the one depicted in Fig. 1, are incorporated in a variety of electronic products where they typically are used for power control. Wire bonding is used to interconnect the internal lands of the package leads to the die and the substrate. In power modules, this interconnection is most commonly done by ultrasonically wedge bonding aluminum wires from bond pads on the die and substrate to bond pads on the module frame that are significantly higher, as shown in Fig. 2.

Power modules, have traditionally been required to survive 1000 thermal cycles between –40°C and +125°C in order to be qualified for use. This procedure is meant to detect module designs that are likely to fail by wire flexural fatigue in field operation, where the wires are subjected to cyclic strain as a result of temperature and power cycling.

This traditional qualification test procedure has several shortcomings. First, the selection of the temperature cycle magnitude and duration is often arbitrary, and the results of the testing are not properly correlated to field life. Second, the procedure is costly and time consuming and is therefore undesirable in today's product development environment of shortened design cycles and quick time-to-market. It is no longer considered best practice to make a prototype, subject it to a series of standardized tests, analyze the failures, fix the design, and test again. A fundamental model that can be used before testing to assess the susceptibility of module designs to wire flexural fatigue is therefore extremely desirable both to minimize testing and to aid in the proper interpretation of the test results. The use of such models to qualify assemblies for field use is known as virtual qualification. This paper presents such a model that can be used to assess the likelihood of wire failure due to cumulative damage resulting from repeated flexure during thermal cycling.

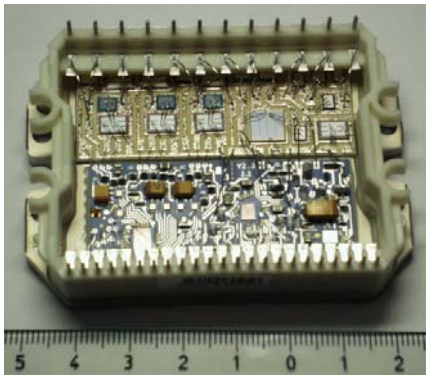

Fig. 1 Hybrid Power Module with the wire bonds used to provide connection between the leads and the substrate.

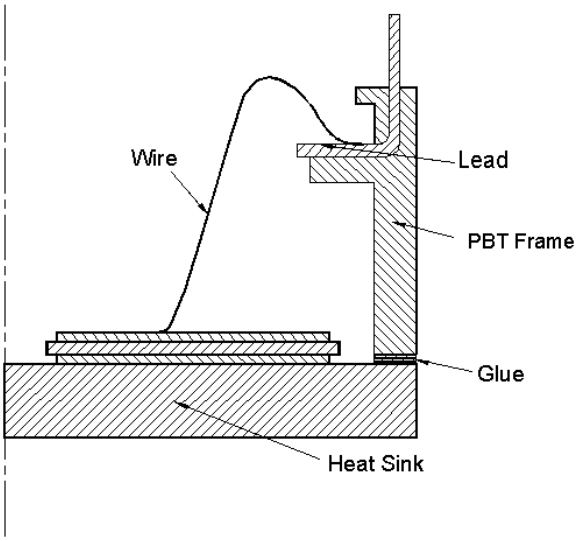

Fig. 2 Outline of a typical wire in a power module.

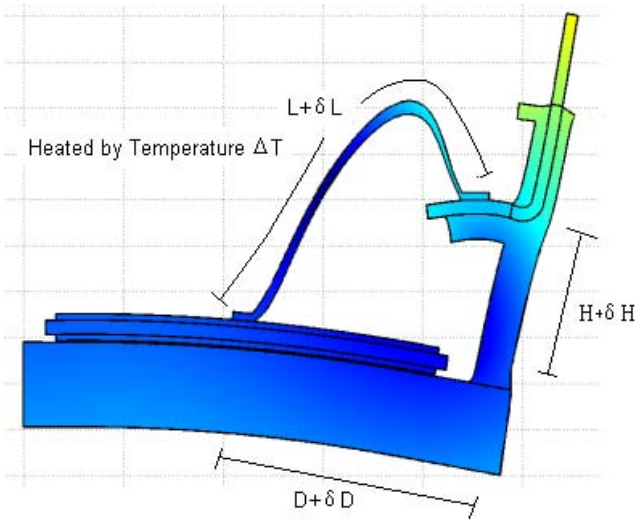

Fig. 3 Wire/frame displacement due to temperature cycling (Not to scale)

Previous analytical models for flexural fatigue of wires have used the theory of bending of elastic curved beams to determine the strains and corresponding stresses. In one model, the stresses are given as a function of the change in the take off angle and the curvature of the wire. These stresses are then placed in Basquin's relation to determine the cycles to failure [1]. The use of this model is limited because of the impracticality of measuring take-off angles. A subsequent model [2] assumed the wire to be a curved beam subjected to pure bending. While this model removes the need to measure take-off angles, it is restricted to modules where the first and second bond pads are at the same height. No models have been developed for the case where aluminum wedge bonds are not at the same height. The model presented in this paper is more general and includes the domain of wirebonded interconnections with a height offset for the bond pads.

MODEL DERIVATION

A wire that is not firmly encapsulated undergoes flexure when subjected to temperature cycling due to the differential thermal expansion between the wire and the substrate and frame, as shown in Fig. 3. This flexure produces stress/strain reversals in the heel of the bond wire [2] that eventually results in fatigue failure of the wire at the upper bond pad, as shown in Fig. 4. Cumulative fatigue damage is induced by these cyclic stress/strain reversals, as observed by the initiation and growth of cracks to fracture. The number of cycles to failure (N_f) is determined by the strain-based power law equation:

$$N_f = C(\varepsilon)^{-m} \tag{1}$$

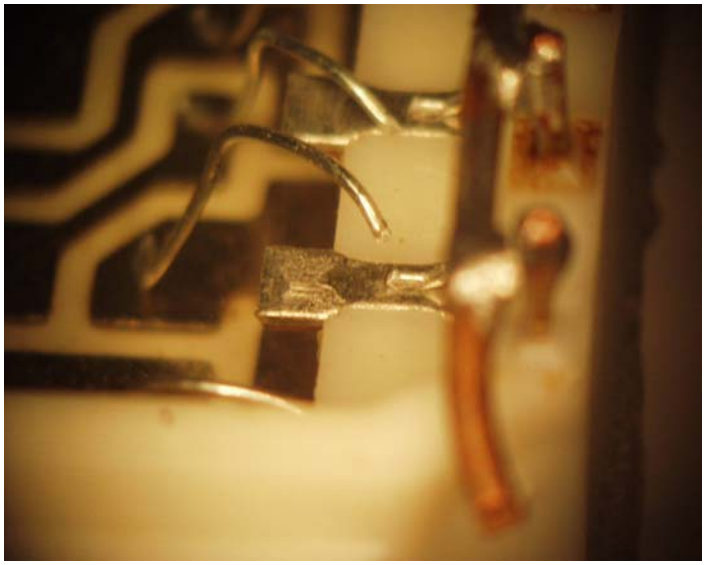

Fig. 4 Typical wire failure due to wire flexure.

Wire Curvature

The theory of curved beams states that the strains at the surface of the concave side of a bent wire are given by the expression,

$$\varepsilon = \frac{(R-\rho)d\psi}{\rho_i \psi_i} = \frac{r(\psi_i - \psi_f)}{\rho_i \psi_i} \tag{2}$$

where R is the radius of curvature of the wire from the centroidal axis of the wire (Fig. 2), ρ is radius of curvature of the wire from the surface of the wire, r is the radius of the cross-section of the wire, ψ is the take-off angle, and the suffixes i and f denote variables described before and after heating of the wire, respectively.

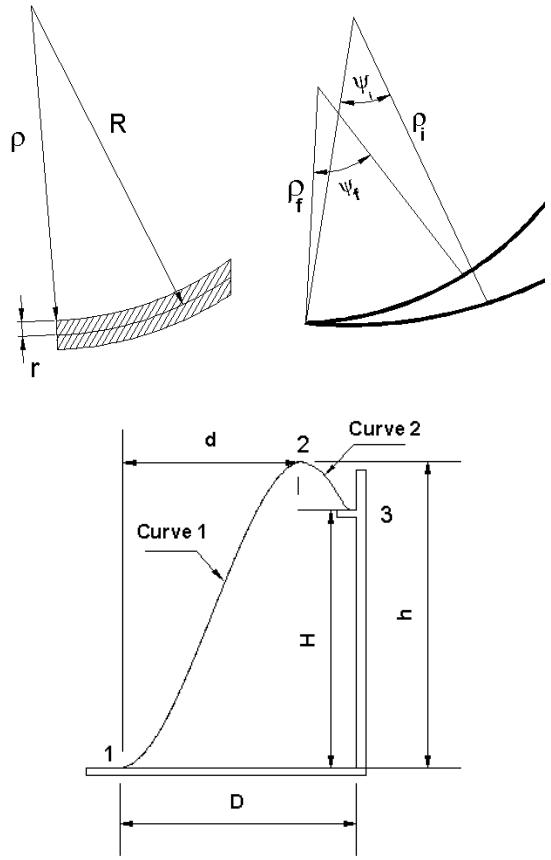

Fig. 5 Wire label definitions.

For the strain expressions on the convex side of the wire (ρ_i+2r) should be used instead of ρ_i, which always results in lower strains and hence lower stresses than the concave side. Therefore, fatigue damage should be greater on the concave side (or top side) of the wire. This is, in fact, where cracks are usually observed to originate.

Assuming there is no appreciable change in the length of a small curved section of the wire, δs, before and after heating we can relate the radii of curvature and the take off angles by the expression:

$$\delta s = \rho_i \psi_i \approx \rho_f \psi_f \tag{3}$$

From Eq. 2 and Eq.3 we can rewrite the expression for the strain as,

$$\varepsilon = \frac{r(\rho_f - \rho_i)}{\rho_i \rho_f} = r(\kappa_i - \kappa_f) \tag{4}$$

κ_i and κ_f are the curvatures of the wire before and after heating, respectively, and they are inversely proportional to the radii of curvature. We see from equation (4) that the strains are a function of the change in curvature. This dependence of wire failures on the wire curvature has also been shown experimentally [3].

Determining the change in wire curvature at the heel of the wire resulting from heating the package requires modeling both the displacement of the bond pads on the module package frame and the changes in wire geometry. The wire geometry can be modeled by fitting it with a piecewise Hermite interpolation polynomial. This approach requires that the co-ordinates of the points 1,2, and 3, shown in Fig. 5, be specified (Note that point 2 defines the actual loop height). The curves $\alpha(u)$ and $\beta(v)$ map the parameters u and v respectively to curve 1 and curve 2 shown in Fig. 5. u and v vary in the open interval (0,1) and are used to represent every point on curves 1 and 2.

$\alpha,\beta: I \rightarrow R^2$ denotes differentiable curves parameterized by u and v respectively such that:

$$\alpha(u) = (ud,\ h(3u^2-2u^3)) \tag{5}$$

$$\beta(v) = (v(D-d)+d,\ h+3(H-h)v^2-2(H-h)v^3) \tag{6}$$

Eq. 5 and Eq. 6 are derived based on the boundary conditions for wedge bonding (i.e. the known values of points 1,2 and 3, and the fact that the slopes are zero at points 1, 2, and 3). For a regular parameterized curve, the curvature $\kappa(u)$ is given by:

$$\kappa(u) = \frac{\left|\alpha(u)' \wedge \alpha(u)''\right|}{\left|\alpha(u)'\right|^3} \tag{7}$$

Substituting u=0 in Eq. 5 defines the curvature of the wire at point 1 while v=1 in Eq. 6 provides the curvature of the wire at point 3 (see Fig. 5).

Simplifying the equations for the curvature, k_{low} (k(u=0)) and k_{high}(k(v=1)) can be written as:

$$\kappa_{low} = \frac{6h}{d^2} \quad , \quad \kappa_{high} = \frac{6(h-H)}{(D-d)^2} \tag{8}$$

The suffixes "low" and "high" represent the values at the lower and higher bond points respectively.

The curvatures given in equation (8) are calculated before and after heating the wire. As the failure is typically observed at the higher bond point, only the difference in curvatures before and after heating at the higher bond point is given,

$$\kappa_i - \kappa_f = \frac{6(h_i - H_i)}{(D_i - d_i)^2} - \frac{6(h_f - H_f)}{(D_f - d_f)^2} \tag{9}$$

The displacement of the bond pads on the package frame due to heating is embedded in the variables D_f, H_f. The values of d_f and h_f are also affected by the wire expansion and frame displacement. They are determined by refitting the wire to a new Hermite polynomial after the heating.

Frame displacement

From Fig. 2 we see that one end of the wire is bonded to a frame while the other end is bonded to the substrate. During module heating, the frame expands and bows displacing the higher bond pads, thus placing additional strain on the wire. An analytical model has been developed to predict the frame displacements. The displacement due to CTE mismatch can be decoupled into a linear motion of the frame and a bending of the frame.

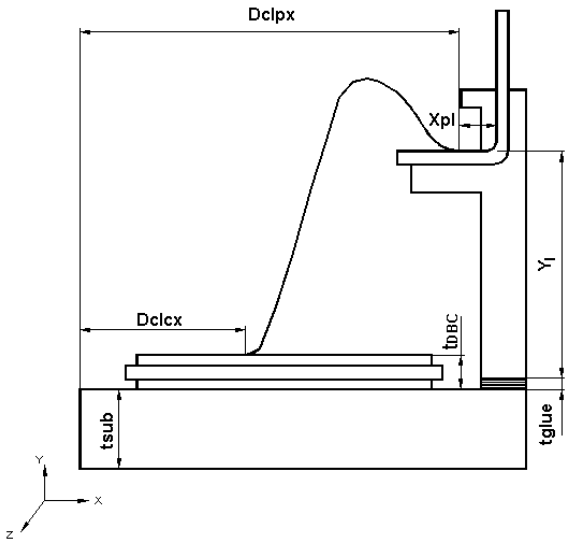

Fig. 6 Frame geometry parameters

For linear displacement due to the rise in temperature ΔT, the span of the bond wire ($D_{x0} = D_{clpx}$-D_{clcx}) increases by:

$$\delta x_l = D_{x0}\alpha_{sub}\Delta T \tag{10}$$

and the bond pad height increases by:

$$\delta y_l = t_{glue}\alpha_{glue}\Delta T + y_1\alpha_{ply}\Delta T - t_{dbc}\alpha_{dbc}\Delta T \tag{11}$$

where α_{sub}, α_{glue}, α_{ply} and α_{dbc} are the thermal expansion coefficients of the power module heat spreader, glue, plastic frame and DBC layers respectively.

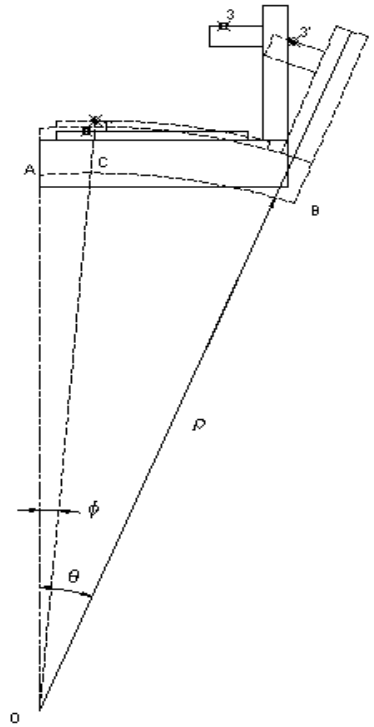

Fig. 7 Bowing of Frame

In addition to the linear displacements, the frame also bows during temperature cycling due to the CTE mismatch of the heat spreader and the DBC layers as shown in Fig. 7. The points 1, 3 and 1', 3' shown in Fig. 7 represent the bond points before and after cooling. The bowing will be significant, considering the length of the heat spreader and substrate and also the CTE mismatch between the layers. The bowing in the frame and substrate has been calculated based on the thickness and corresponding material properties of the layers using the method of Timoshenko [4] as applied by Neugebauer [5]. The displacement in the center of the bow is given by:

$$Ss = \frac{3\left(D_{clpx} + x_{pl}\right)^2\left(\alpha_{sub} - \alpha_{dbc}\right)\Delta T}{t_{sub}}(F) \tag{12}$$

where

$$F = \frac{(1+m)}{3(1+m)^2 + (1+mn)\left[m^2 + \frac{1}{mn}\right]} \tag{13}$$

$$m = \frac{t_{dbc}}{t_{sub}} \quad , \qquad n = \frac{E_{dbc}}{1-\nu_{dbc}}\frac{1-\nu_{sub}}{E_{sub}} \tag{14}$$

where ν is the Poisson's ratio, E is the modulus of elasticity and t is the thickness of corresponding layers. Subscripts "dbc" and "sub" denote the DBC substrate and the heat spreader layers, respectively.

The radius of curvature of bowing of the frame is very large compared to the dimensions of the frame. Also, the bowed frame subtends a very small angle at the center , so the simplifying assumption can be made that $\cos(\theta)=1 - \theta^2/2$; $\sin(\theta)=\theta-\theta^3/6$). From the arc length, AB, shown in Fig. 7 , it can be easily proved that,

$$\theta = \frac{2Ss}{\text{Arc Length AB}} \qquad \rho = \frac{\text{Arc Length AB}}{\theta} \tag{15}$$

$$\phi = \frac{\text{Arc Length AC}}{\rho} \tag{16}$$

The net change in displacements due to bowing is given by:

δx_b=difference in x-co-ordinate of 3' & 1' – difference in x-co-ordinate of 3 & 1

$$=[(\rho+t_{sub}+t_{glue}+y_l)\sin\theta - x_{pl}\cos\theta - (\rho+t_{sub}+t_{dbc})\sin\phi] - [D_{clpx}-D_{clcx}] \tag{17}$$

δy_b=difference in y-co-ordinate of 3' & 1' – difference in y-co-ordinate of 3 & 1

$$=[(\rho+t_{sub}+t_{glue}+y_l)\cos\theta + x_{pl}\sin\theta - (\rho+t_{sub}+t_{dbc})\cos\phi] - [y_l+t_{glue}-t_{dbc}] \tag{18}$$

The displacements shown in Eq. 10, Eq. 11, Eq. 17 and Eq. 18 take into account the effect of movement of frame due to heating. The new values of D_f and H_f are given by,

$$D_f = D_i + \delta x_b + \delta x_l \quad , \qquad H_f = H_i + \delta y_b + \delta y_l \tag{19}$$

Strains and stresses at the heel of the bond wire

Using the calculations of the frame displacement and the expansion of the wire due to heating, the new curvatures are also calculated. Using Eq. 4, and Eq. 8 the strains of the wire are given by:

$$\varepsilon_{low} = \frac{6r(d_f^{\,2}h_i - d_i^{\,2}h_f)}{d_i^{\,2}d_f^{\,2}}$$
$$\varepsilon_{high} = \frac{6r\left((D_f - d_f)^2(h_i - H_i) - (D_i - d_i)^2(h_f - H_f)\right)}{(D_i - d_i)^2(D_f - d_f)^2} \quad (20)$$

If we assume linear elastic behavior we could calculate the stresses by the following expressions:

$$\sigma_{low} = \frac{6Er(d_f^{\,2}h_i - d_i^{\,2}h_f)}{d_i^{\,2}d_f^{\,2}}$$
$$\sigma_{high} = \frac{6Er\left((D_f - d_f)^2(h_i - H_i) - (D_i - d_i)^2(h_f - H_f)\right)}{(D_i - d_i)^2(D_f - d_f)^2} \quad (21)$$

However, for high temperature load cycles that cause the wire to yield, the Hooke's law becomes invalid. In such cases, the strains shown in Eq 20 are used for life prediction. These are total strains but are approximately equal to the plastic strains for a very high load case.

Life Prediction Model of the Wire

Wires typically exhibit low cycle fatigue behavior (N_f < 3000 cycles) at the high ΔT that power modules experience during typical temperature cycling tests. Therefore, a strain-based Coffin-Manson relation (i.e. $N_f = C\varepsilon^{-m}$) is appropriate for life prediction of the wire. The total strain in the wire can be written in terms of the plastic and elastic strains as

$$\varepsilon = \varepsilon_{plastic} + \varepsilon_{elastic} \quad (22)$$

For the high load cycle that the modules experienced, the plastic strains were much higher than the elastic strains. For simplicity in the model, the total strains were assumed approximately equal to the plastic strains. However, this approximation does not hold good for cases when the plastic strains are small. This problem could be overcome by applying the load in steps in order to partition the elastic strains from the plastic strains. This approach would be demonstrated in a forthcoming paper to be presented by the authors at the forthcoming ASME congress, held in Washington DC in November 2003. For a low-cycle fatigue model, the fatigue constant values (defined in Eq. 1) for the identical Al alloy were found in the literature to be C= 1.0 and m=1.4 [6,7].

Underlying Assumptions in the Model

1. The model is two dimensional in nature and any co-ordinates in the z-direction must be mapped onto a two dimensional plane. Therefore, the model does not account for twisting in the wires.
2. Considering the high load cycles applied, the total strains have been approximated to be equal to the plastic strains. These strains are then used in the Coffin-Manson based relation to predict the cycles to failure.
3. The model does not account for pre-stressing in the wire due to the manufacturing process.

Validation against Hu-Pecht-Dasgupta Model

The Hu-Pecht-Dasgupta model [2] predicts the heel stresses for a wire that is bonded without a height offset (H=0). The stresses are given by:

$$\sigma = 6E\frac{r}{D'}\left(\frac{L'}{D'} - 1\right)^{0.5}\left(2\alpha_s + \frac{\alpha_s - \alpha_w}{1 - D'/L'}\right)\Delta T \quad (23)$$

where, α_w & α_s are the coefficients of thermal expansion of the wire and substrate respectively, E is the modulus of elasticity, r is the radius of the wire and L' & D' are the half-lengths and half-span of the wire respectively.

It is seen from Fig. 8 that the output from the current model matches closely with the Hu-Pecht-Dasgupta model.

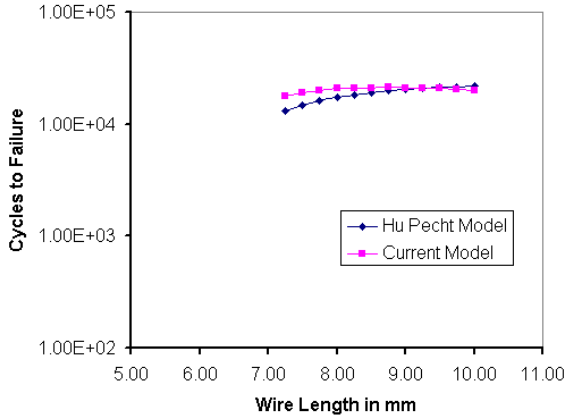

Fig. 8 Validation against the Hu-Pecht-Dasgupta Model

EXPERIMENTAL VALIDATION

Five modules similar to the one shown in Fig. 1 were subjected to liquid-to-liquid thermal shock from –40°C, to 125°C. The wire bonds were assigned values 1-12 counting from left to right, as shown below in Fig. 9.

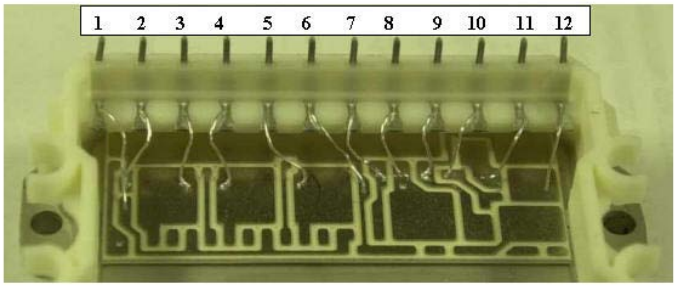

Fig. 9 Module with the Bond # shown

One cycle consisted of 5 minutes in the cold bath to bring the module temperature to –40° C, followed by 3 minutes in the hot bath to bring the module temperature to 125° C. The transit time between baths was approximately 5 seconds in ambient air at 25° C. The temperature profile is shown in Fig. 10.

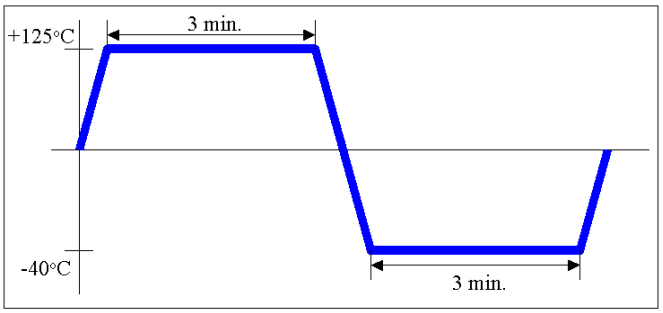

Fig. 10 Thermal Cycling Load Profile

After each test, all the wire bonds on each of the modules were tested for continuity using a multimeter as well as visual inspection. The location of failure for each wirebond was photographed to document the failure site and failure mode. Every wirebond failed at the heel of the wedge bond to the upper bond pad. No wires exhibited bond lift-off, and all bonds to the DBC remained intact. The failure site of a wirebond, after 1125 cycles is shown in Fig. 4.

The number of cycles to flexural fatigue failure for each wire was used to validate the output from the model. The experimental results and theoretical values from the model are compared in Fig. 11.

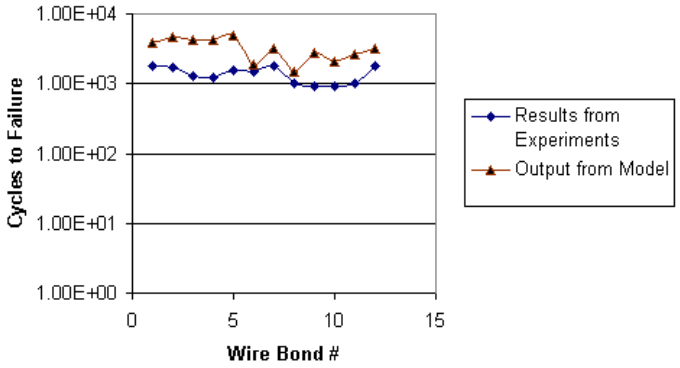

Fig. 11 Comparison of output from Model and Experiment

DISCUSSION

This model permits the user to determine the acceleration factor for flexure fatigue of different diameter aluminum wires in various designs and layouts. This allows the further determination of the field life of the wire at different operating and environmental application conditions based on the acceleration factor and a known time to failure for a given test condition.

A special feature of the model is the ability to assess the susceptibility of wires to flexure fatigue based solely on the wire span, loop height, and downbond. There is no necessity to determine the wire take-off angle, the wire radius of curvature, or even the wire length – all of which are difficult to measure in practice. It is also the first model to fully include the effects of expansion and bowing of the frame on the reliability of the wire. In addition, this model can be used for both high and low cycle wire fatigue caused by elastic and plastic strain cycling, respectively.

A plot of the time to failure as a function of the temperature cycle magnitude is given in Fig. 12 for the following wire geometry:

Wire span: 4 mm
Wire height: 7.7 mm
Downbond offset: 6.3 mm

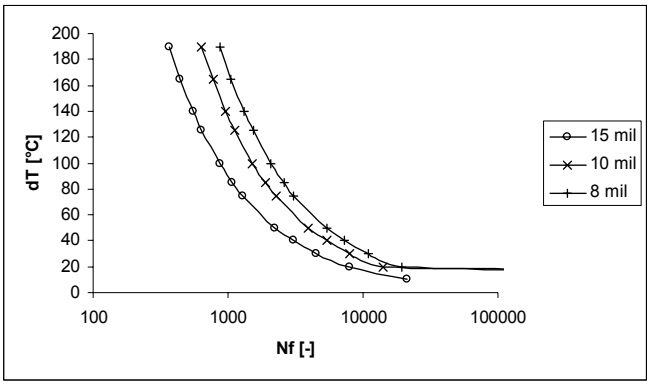

Fig. 12 Wire life as a function of Temperature

As seen in the figure, the time to failure increases steadily as the temperature cycle magnitude is decreased until a magnitude of about $\Delta T = 30°C$ for a 8 mil wire and $\Delta T=10°C$ for a 15 mil wire. At that point, the strain becomes fully elastic and then the time to failure increases drastically as very little damage is done to the wire in each elastic strain-reversal cycle. This drastic increase in the time-to-failure can be considered an endurance limit for this wire. This prediction of a much higher time to failure for elastic strains is based on experimentally determined elastic fatigue coefficients for the wire. In this high cycle, fully elastic fatigue range ($Nf > 3 \times 10^4$, Nf – Number of cycles to failure), a stress-based model (Basquin's Power Law), is used to relate the stresses to the number of cycles to failure.

$$N_f = C_1 \sigma^{-C2} \quad \text{(Eq. 24)}$$

where C_1 and C_2 are elastic fatigue constants of the wire, and σ is measured in MPa. The fatigue constants have been determined for an 8 mil and a 15 mil wire using an MTS Tytron micro-fatigue tester.

The fatigue constants for 8 mil wire are $C_1 = 3.846 \times 10^{23}$ and $C_2=10.34$ whereas for the 15 mil wire, they are $C_1= 3.57273 \times 10^{25}$ and $C_2 = 11.54$. The prediction of a long life for failure by this elastic wire flexure fatigue model is supported by the fact that modules subjected to temperature cycle magnitudes in this range, induced by power cycling, fail by an alternate failure mechanism, wire liftoff resulting from solder fatigue and temperature overstress, between 20,000 cycles and 200,000 cycles, instead of by flexure fatigue. This failure mechanism shift, however, makes it impossible to determine exactly how long it would take for the wires to fail in flexure using the actual modules, thereby making it difficult to validate the actual predictions of the model in this range.

It is observed that the model gives a conservative result in the plastic strain range. This is largely due to the underlying assumptions used in the model. Also, the model assumes that the coordinates that define the wire geometry are very accurate, especially the highest point of the wire (Point 2 defined in Fig. 5). This dependence on the accurate location of point 2 is seen in Fig. 13. However, from a design point of view, the model seems appropriate, given the small change in lifetime when the

reference point is defined with a tolerance of +/-0.5 mm, as demonstrated in Fig. 14.

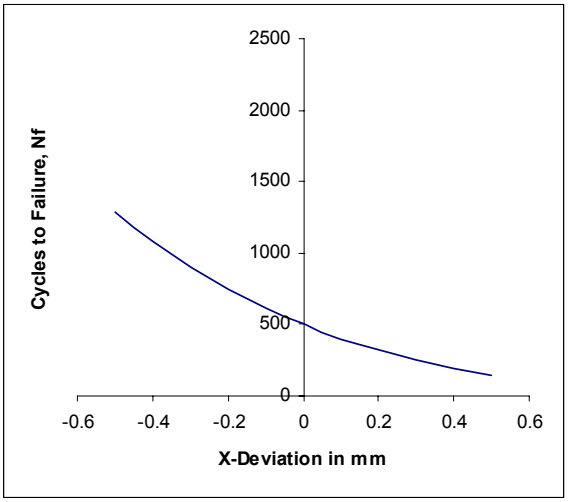

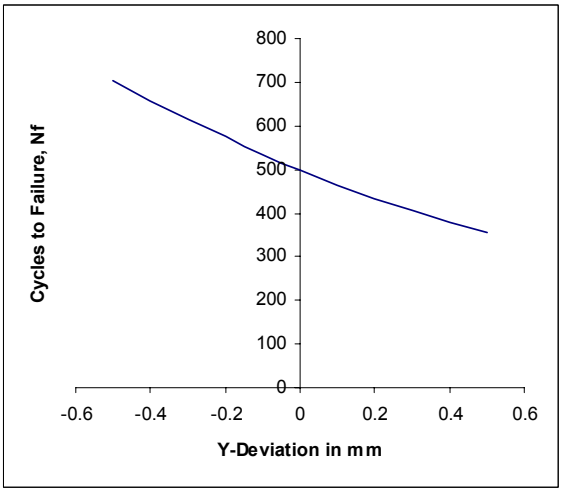

Fig. 13 Variation in model output due to variation of top point definition.

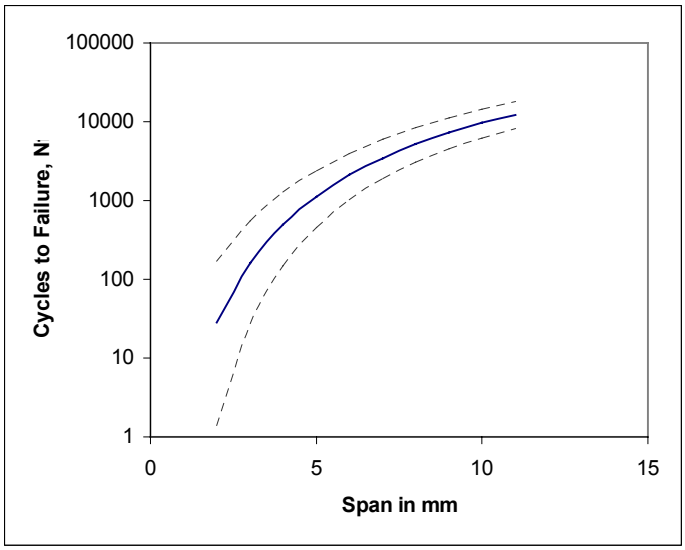

Fig. 14 Dependence of wire lifetime on wire span. The variation in lifetime for a ±0.5mm tolerance in the location of point 2 is indicated by the dotted lines.

The differences between the theoretical predictions of the model and the experimental results maybe attributed to several factors not considered in the model such as twisting of the wires, wire thinning near the heel, and prestressing due to the wire bonding process. Any small variations in the strains/stresses then get magnified when the cycles to failure are computed, since the Coffin-Manson and Basquin's relations have power law formulations. Nevertheless the model captures the trend observed in the field, though the cycles to failure are on the conservative side. Currently, work is being done to include an energy-based approach to design wire/wirebonds interconnections.

CONCLUSIONS

A model has been constructed to predict the cycles to failure by wire flexural fatigue in power modules. The model uses a Hermite interpolation scheme to fit the wire geometry with only wire span, loop height, wire diameter, and downbond needed to fully describe the wire geometry. The model combines both changes in the wire geometry and changes in the frame geometry as a function of temperature cycling to calculate the strains in the heel of the wire. These strains are converted to a time to failure using elastic and plastic damage models. This model can act as a good design evaluation tool to predict the cycles to failure for an existing or proposed design if precise measurements of the reference points are used.

ACKNOWLEDGMENTS

The authors would like to thank the over 30 members of the CALCE Electronic Products and Systems Consortium for their support of this research and particularly Grundfos Management A/S for its technical and financial leadership. The authors would also like to thank the MINVA project sponsored by the Danish Energy Council, Grundfos, Electrolux, and Aalborg University, and the AEPS project (Contract #N009814823) sponsored by the Office of Naval Research for

their support of our power electronics reliability efforts. Finally, the authors express their gratitude to Mr. Zeke Topolosky and Mr. Witaly Zeiler for their assistance with the validation testing.

NOMENCLATURE

ε = Strain at the wire heel due to wire flexure
σ = Stress at the wire heel due to wire flexure
C = Plastic fatigue constant for the wire
m = Plastic fatigue exponent for the wire
C_1, C_2 = Elastic fatigue constants for the wire
R = Radius of curvature from the centroidal axis
r = Radius of wire
ρ_i = Radius of curvature before heating
ρ_f = Radius of curvature after heating
ψ_i = Take off angle before heating
ψ_f = Take off angle after heating
κ_i = The curvature at the heel of the wire before heating
κ_f = The curvature at the heel of the wire after heating
$\alpha(u)$ = Differentiable curve parameterized by u
$\beta(v)$ = Differentiable curve parameterized by v
d_i = The x co-ordinate of the reference point, defining the loop height, before heating
h_i = The y co-ordinate of the reference point, defining the loop height, before heating
D_i = The span of the wire before heating
H_i = The bond pad height offset of the wire before heating
d_f = The x co-ordinate of the reference point, defining the loop height, after heating
h_f = The y co-ordinate of the reference point, defining the loop height, after heating
D_f = The span of the wire after heating
H_f = The bond pad height offset of the wire after heating
δx_l = The x frame displacement due to bowing of frame
δy_b = The y frame displacement due to bowing of frame
t_{sub} = Thickness of the heat spreader
t_{glue} = Thickness of the glue in the power module
t_{dbc} = Thickness of the DBC layer
D_{clcx} = Distance of first bond point from the center of the power module
D_{clpx} = Distance of second bond point from the center of the power module
Ss = Displacement in the center of the bow
α_{sub} = Thermal expansion coefficient of the heat spreader
α_{glue} = Thermal expansion coefficient of the glue
α_{ply} = Thermal expansion coefficient of the plastic frame
α_{dbc} = Thermal expansion coefficient of the DBC layer
E = Modulus of elasticity of Al wire
L' = Half length of wire
D' = Half span of wire
ΔT = Temperature load cycle applied

REFERENCES

1. Pecht, M., Dasgupta, A., and Lall, P., 1989, “A failure prediction model for wire bonds”, ISHM proceedings, pp 607-613.
2. Hu, J. M., Pecht, M., and Dasgupta, A., 1991, “A probabilistic approach for predicting thermal fatigue life of wire bonding in microelectronics”, Journal of Electronic Packaging, vol. 113, pp 275-285.
3. Ramminger, S., Seliger, N., and Wachutka, G., 2000, “Reliability Model for Al Wire Bonds subjected to Heel Crack Failures”, Microelectronics Reliability, vol 40, pp 1521-1525.
4. Timoshenko, S., 1925, “Analysis of Bi-Metal Thermostats”, Journal of Optical Society of America, vol. 23, pp. 233-55.
5. Neugebauer, C. A., Yerman, A. F., Carlson, R. O., Burgess, J. F., Webster, H. F., and Glascock, H. H., 1986, “The Packaging of Power Semiconductor Devices-Vol 7”, Gordon and Breach Science Publishers.
6. Deyhim, A., Yost, B., Lii, M. J., and Li, C. Y., 1991, “Characterization of the fatigue properties of bonding wires”, Electronic Components and Technology Conference, pp 836-841.
7. Suresh, S., 1998, “Fatigue of Materials”, Cambridge University Press, Second Edition.